forests

MDPI

Article

Assessment of the Spatiotemporal Dynamics of Suitable Habitats for Typical Halophytic Vegetation in China Based on Maxent Model and Landscape Ecology Theory

Fuyin Guo [1,2,3], Xiaohuang Liu [1,2,4,*], Xuehua Chen [5], Hongyu Li [1,4], Zulpiya Mamat [3], Jiufen Liu [1,4], Run Liu [1,4], Ran Wang [1,4], Liyuan Xing [1,4] and Junnan Li [1,4]

1 Key Laboratory of Coupled Processes and Effects of Natural Resources Elements, Beijing 100055, China; 107552203685@stu.xju.edu.cn (F.G.); lihongyu@mail.cgs.gov.cn (H.L.); liujiufen@mail.cgs.gov.cn (J.L.); liurun6046@163.com (R.L.); wangran@mail.cgs.gov.cn (R.W.); xingliyuan@mail.cgs.gov.cn (L.X.); lijunnan@mail.cgs.gov.cn (J.L.)
2 Key Laboratory of Groundwater Sciences and Engineering, Ministry of Natural Resources, Beijing 100055, China
3 College of Geography and Remote Sensing Science, Xinjiang University, Urumqi 830017, China; zulpiya1219@sina.com
4 Natural Resources Comprehensive Survey Command Center, China Geological Survey, Beijing 100055, China
5 Xinjiang Academy of Surveying and Mapping, Urumqi 830017, China; xuehuachen2023@163.com
* Correspondence: 15313256806@163.com

Abstract: The widespread and complex formation of saline soils in China significantly affects the sustainable development of regional ecosystems. Intense climate changes and regional land use further exacerbate the uncertainties faced by ecosystems in saline areas. Therefore, studying the distribution characteristics of typical halophytic vegetation under the influence of climate change and human activities, and exploring their potential distribution areas, is crucial for maintaining ecological security in saline regions. This study focuses on *Tamarix chinensis*, *Tamarix austromongolica*, and *Tamarix leptostachya*, integrating geographic information systems, remote sensing, species distribution models, and landscape ecological risk (LER) theories and technologies. An optimized MaxEnt model was established using the ENMeval package, incorporating 143, 173, and 213 distribution records and 13 selected environmental variables to simulate the potential suitable habitats of these three *Tamarix* species. A quantitative assessment of the spatial characteristics and the area of their potential geographical distribution was conducted. Additionally, a landscape ecological risk assessment (LERA) of the highly suitable habitats of these three *Tamarix* species was performed using land use data from 1980 to 2020, and the results of the LERA were quantified using the Landscape Risk Index (LERI). The results showed that the suitable areas of *Tamarix chinensis*, *Tamarix austromongolica*, and *Tamarix leptostachya* were 9.09×10^5 km^2, 6.03×10^5 km^2, and 5.20×10^5 km^2, respectively, and that the highly suitable habitats for the three species were concentrated in flat areas such as plains and basins. *Tamarix austromongolica* faced increasing ecological risk in 27.22% of its highly suitable habitat, concentrated in the northern region, followed by *Tamarix chinensis* in 16.70% of its area with increasing ecological risk, concentrated in the western and northern highly suitable habitats; *Tamarix chinensis* was the least affected, with an increase in ecological risk in only 1.38% of its area. This study provides valuable insights for the protection of halophytic vegetation, represented by *Tamarix*, in the context of China's national land development.

Keywords: halophytic; *Tamarisk*; MaxEnt; landscape ecological risk assessment; spatiotemporal variation

Citation: Guo, F.; Liu, X.; Chen, X.; Li, H.; Mamat, Z.; Liu, J.; Liu, R.; Wang, R.; Xing, L.; Li, J. Assessment of the Spatiotemporal Dynamics of Suitable Habitats for Typical Halophytic Vegetation in China Based on Maxent Model and Landscape Ecology Theory. *Forests* **2024**, *15*, 1757. https://doi.org/10.3390/f15101757

Academic Editors: Aqil Tariq and Leila Hashemi Beni

Received: 10 September 2024
Revised: 3 October 2024
Accepted: 4 October 2024
Published: 6 October 2024

1. Introduction

Soil salinization has become a major environmental and socio-economic issue worldwide. With the intensification of climate change and human activities, this situation is expected to worsen, severely impacting regional ecological security and sustainable development [1]. Halophytes, which account for 1%–2% of all terrestrial plant species, play a crucial role in sustaining regional ecosystems [2]. Salt-tolerant plants have adapted to survive under saline conditions through special osmotic regulation mechanisms or salt excretion systems, such as ion compartmentalization into vacuoles or the junction of roots and stems to prevent ions from reaching above-ground parts. These adaptations allow them to grow in high-salinity soil [3]. Halophytic vegetation is ecologically dominant in arid and semi-arid environments. However, due to the fragile ecological conditions in these regions and the impact of human activities, species loss is significantly higher than in areas with more diverse vegetation [4]. In response to the challenges faced by halophytic vegetation, various countries have enacted laws and allocated resources to protect these plants [5]. At present, both establishing natural reserves focused on halophytes and creating germplasm repositories are beneficial for their protection. In this context, exploring the current distribution of halophytic vegetation and suitable habitats is of practical significance.

Tamarisk is one of the few native shrub species widely distributed in arid and semi-arid saline areas, commonly found along riversides, coastal regions, sandy lands, and saline–alkali areas. It is considered an excellent halophyte for restoring saline soils and is a key component of China's "Southern Redwoods and Northern Willows" ecological project [6]. To adapt to complex high-salt environments, *Tamarisk* has evolved specialized salt-excreting structures—salt glands. These glands allow *Tamarisk* to secrete excess salt, preventing excessive salt absorption [7]. Salt in the dead branches and fallen leaves often adheres to sand grains, forming "*Tamarisk* sandbags". Tamarisk exhibits characteristics such as salt resistance, drought resistance, wind protection, sand fixation, and soil improvement, playing a crucial role in maintaining the stability of saline–alkali land ecosystems [8]. Therefore, faced with increasing soil salinization and ecological security risks, exploring the distribution patterns of suitable habitats for *Tamarix* in China and associated ecological risks will aid in developing protection strategies for dominant halophytic vegetation and conservation plans for germplasm resources, improving salinized soils, and maintaining the ecological security of the environment.

Ecological niche models (ENM) use algorithms to analyze species' actual distribution areas and potential geographical locations by considering their current range and environmental variables [9]. Among various species distribution models, the MaxEnt model has higher accuracy in predicting results, less demand for sample size and environmental variables, low sensitivity to sample bias [10], and has been proven to have better results in recent years in practice [11–13]. Current research using the MaxEnt model primarily focuses on natural factors such as climate and altitude, making it challenging to assess the impact of human activities at the land-use scale. However, recent studies have shown that human activities significantly affect *Tamarix* species' habitats, and these impacts must be considered [4,14]. This study integrates the MaxEnt model with landscape theory to comprehensively assess the spatiotemporal distribution patterns of *Tamarix* habitats. We focused on three *Tamarix* species—*Tamarix chinensis*, *Tamarix austromongolica*, and *Tamarix leptostachya*—incorporating recent research and using machine learning methods and landscape ecology principles to support *Tamarix* conservation. The specific objectives are as follows: (1) to analyze the spatial patterns of potential suitable habitats for the three *Tamarix* species and quantify the core suitable habitats; (2) to assess the ecological risk of these habitats and identify risk areas; and (3) to analyze the characteristics of the spatial distribution of risk areas in the highly suitable areas for three types of *Tamarisk* based on the landscape ecological risk index.

2. Materials and Methods

2.1. Data Collection and Preprocessing

2.1.1. Acquisition and Selection of Species Location Information

This study examined three species of *Tamarix* plants: *Tamarix chinensis*, *Tamarix austromongolica*, and *Tamarix leptostachya*. The location data was collected through (1) field investigations conducted in the Taklimakan Desert, Xinjiang from 2023 to 2024; (2) a review of relevant literature and a collection of *Tamarix* distribution records [15–18]; and (3) searches of the Global Biodiversity Information Facility database (https://www.gbif.org/ (accessed on 13 March 2024) GBIF Occurrence Download https://doi.org/10.15468/dl.hc4hhd), National Specimen Platform ((Accessed 13–15 March 2024) http://www.nsii.org.cn), Chinese Virtual Herbarium ((Accessed 15–18 March 2024) https://www.cvh.ac.cn), and China National Specimen Museum ((Accessed 19–21 March 2024) https://cfh.ac.cn).

These methods produced 56, 118, and 386 records of occurrence locations for the three *Tamarisk* species, respectively. For specimens lacking precise geographic coordinates, the longitude and latitude were determined using specimen location information and Google Earth, removing distribution points with vague descriptions or duplicate coordinates. Spatial sparsity methods were employed to minimize the spatial autocorrelation between the sample points, and records before 1980 were excluded. This process resulted in 213 records for *Tamarix chinensis*, 173 for *Tamarix austromongolica*, and 143 for *Tamarix leptostachya* (Figure 1).

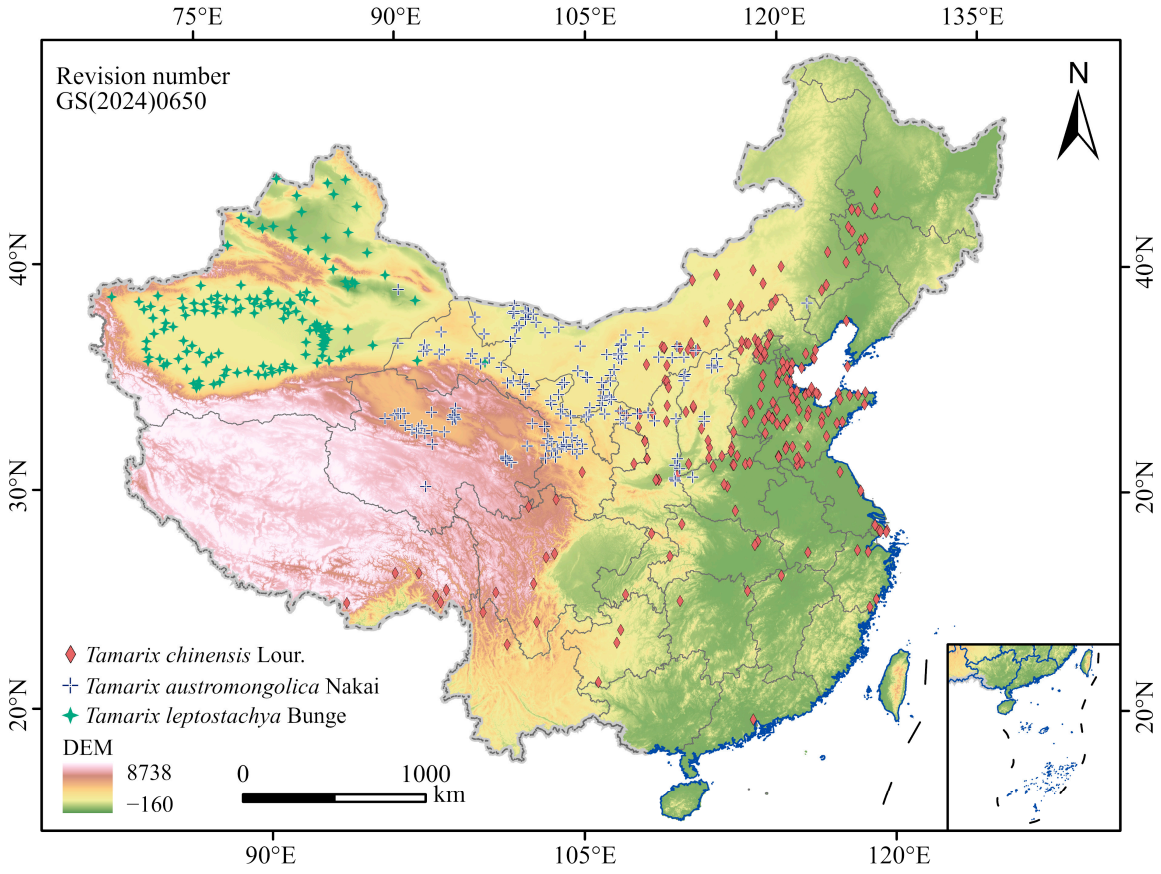

Figure 1. Distribution records of the three species of *Tamarix* L. we screened for.

2.1.2. Data Sources and Preprocessing

Initially, 127 environmental variables were selected for analysis, including bioclimatic, soil, topographic, and sunshine duration data (Table 1). The bioclimatic and elevation data were obtained from the WorldClim dataset version 2.1 ((Accessed 11 March 2024) https://worldclim.org/) [19], with a spatial resolution of 1 km and including 19 variables such as

temperature and precipitation. The high-resolution national soil information grid for China was sourced from the Tibetan Plateau Data Center (2010–2018; (Accessed 9 March 2024) https://data.tpdc.ac.cn/). The China land use dataset and administrative boundary data were obtained from the Resource and Environmental Science and Data Center ((Accessed 12 March 2024) https://www.resdc.cn/). Road and water system data were acquired from the OpenStreetMap data platform ((Accessed 12 March 2024) https://openmaptiles.org/).

Table 1. Research data.

Datasets	Description and Variables	Spatial Resolution (m)	Available Period
WorldClim 2.1	WorldClim is a climate dataset widely used in ecological modeling research, which includes 19 indicators related to temperature and precipitation.	1000	1970–2000
Basic soil property dataset of high-resolution China Soil Information Grids	The dataset consisted of (0–5 cm, 5–15 cm, 15–30 cm, 30–60 cm, 60–100 cm, and 100–200 cm) soil organic carbon, pH, total nitrogen, total phosphorus, total potassium, cation exchange, gravel content (>2 mm), sand, silt, clay, soil texture type, bulk weight, and soil body thickness, and 105 other variables.	1000	2010–2018
Copernicus DEM	Based on the COP-DEM data, the topographic metrics (e.g., slope gradient and slope direction) were extracted. Other topographic properties(i.e., slope, aspect, hillshade)were calculated in ArcGISPro3.1.	30	~
China Multi-period Land Use Remote Sensing Monitoring Data Set (1980–2020)	The CNLUCC dataset was based on Landsat remote sensing images and was constructed through manual vision of land use in China. The land use is classified into six primary categories: cultivated land, forest land, grassland, water area, construction land, and unused land.	1000	1980–2020
HydroRIVERS	The HydroRIVERS dataset is the vector data of the global river network, including features such as river order and river reach length. Generation of distance to river data based on ArcGISPro3.1.	~	~

To address potential issues of autocorrelation and multicollinearity among different variables, this study employed the Pearson correlation coefficient and the jackknife method for variable selection [20]. Variables with a correlation coefficient below 0.8 and a high contribution to the model were selected for further analysis [21].

2.2. Research Method

In this paper, we assessed the habitat suitability of three *Tamarisk* species based on the MaxEnt model using rainfall and administrative data as constraints to delineate the highly suitable habitats for each *Tamarisk* species; based on this, we carried out a landscape ecological risk assessment, analyzing the ecological risk of the three *Tamarisk* species in each core area through trend analysis and significance tests.

2.2.1. Model Analysis and Verification

The model data were resampled using the nearest neighbor method with a uniform raster data resolution of 1 km. During the MaxEnt modeling process, we used 25% of the species distribution points as the test set and 75% as the training set. To avoid overfitting, we optimized the MaxEnt model using 60 sets of regularized multipliers (RM) and feature combinations. The RM values ranged from 0.5 to 6 with an increment of 0.5, and we used five feature combinations (FC): L, LQ, LQH, LQHP, and LQHPT (linear (L), quadratic (Q), hinge (H), product (P), and threshold (T)) [22]. During the MaxEnt model building process, the

average of 10 model runs was taken, with the importance of each variable assessed using the jackknife method, and the response curves were generated [23]. Based on expert knowledge, the suitability results for the Tamarix habitats are categorized into four groups: unsuitable (<0.2), low suitability (0.2–0.4), medium suitability (0.4–0.6), and high suitability (0.6–1) [24].

The receiver operating characteristic (ROC) curve is a key method for evaluating potential species distribution models [25]. The area under the curve (AUC), which ranges from 0 to 1, is used to assess the model's predictive performance. A larger area under the ROC curve indicates better predictive ability [26]. The AUC evaluation criteria are not significant ($0 < AUC \leq 0.5$), poor ($0.5 < AUC \leq 0.7$), moderate ($0.7 < AUC \leq 0.8$), good ($0.8 < AUC \leq 0.9$), and excellent ($0.9 < AUC \leq 1$).

2.2.2. Landscape Pattern Index

To conduct a LERI, it is first necessary to delineate landscape boundaries. When studying suitable habitats for three Tamarix species, challenges include overlapping suitable habitats for different species and excessively large geographical unit ranges for the habitats of a particular species. To address this, we will us the high suitability areas predicted by the MaxEnt model as a baseline, apply precipitation and administrative boundaries as constraints to delineate suitable habitats, and compare raster values where habitats for different Tamarix species overlap. This process helps to delineate overlapping areas and ultimately identify potential core suitable habitats for each species.

Using a grid as an evaluation unit is a viable method for LERI. Based on previous research and comparative experiments, we will divide the study area into 10 km × 10 km grid cells specifically for LERI research [27]. Formula (1) was used to determine the LERI for each risk grid and assign the centroid values to the grids. Then, Kriging was used to interpolate these values to generate a continuous geographic spatial distribution of LERI. LERI is closely related to the region's ability to resist external disturbances [28]. In simple terms, a higher LERI value indicates weaker resistance to disturbances, while a lower risk value signifies stronger resilience of the landscape. Given this, we plan to use the landscape vulnerability index and landscape disturbance index to calculate the LERI of the study area [29], with the formula as follows:

$$LERI = \sum_{i=1}^{n} \frac{A_{ki}}{A_k} \times R_i \quad (1)$$

In this formula, n represents the number of landscape types within the study unit; A_{ki} denotes the area of landscape type i in study unit k; S_k represents the area of study unit k; and R_i is the landscape loss index.

$$R_i = V_i \times E_i \quad (2)$$

V_i represents landscape vulnerability, which is used to describe the stability within the landscape; E_i is the disturbance index, which describes the landscape's resistance to disturbances. Combining the actual conditions of the study area, this study has ranked the vulnerability of different land use types from low to high as follows: construction < woodland < grassland < cropland < water < unused, and assigned values of 1, 2, 3, 4, 5, 6, respectively. Different land use types are normalized according to these assigned values to obtain the weights of each land category. E_i is obtained by calculating the weighted average of the landscape fragmentation (C_i), landscape separation (S_i), and landscape dominance (D_i) of landscape type i:

$$E_i = aC_i + bN_i + cF_i \quad (3)$$

$$C_i = \frac{n_i}{A_i} \quad (4)$$

$$N_i = \frac{A}{2A_i} \times \sqrt{\frac{n_i}{A_i}} \quad (5)$$

$$F_i = \frac{2ln(P_i/4)}{lnA_i} \quad (6)$$

In this formula, a, b, and c represent the weights of C_i, N_i, and F_i, respectively, and their values are set to 0.5, 0.3, and 0.2 based on existing research and the actual conditions of the study area [30]; N_i is the number of patches of landscape type i and A_i is the total area of landscape type i.

2.2.3. Trend Analysis and Significance Testing

The Theil–Sen Median method is a robust linear regression method. This method is highly stable and computationally efficient, and it can reduce the influence of outliers on the results. It is a non-parametric technique used to estimate linear trends [31]. The formula is as follows:

$$\beta = \text{Median}(\frac{x_j - x_i}{j - i}), 1 \leq i < j \leq n \quad (7)$$

In this formula, x_i to x_j represents the values of LERI in different years and median() represents the median operation. If β is less than 0, it indicates that LERI shows a decreasing trend over time; conversely, it signifies an increasing trend.

The Mann–Kendall (MK) test is a non-parametric method used for detecting trends in time series data. It is not affected by missing values and outliers, which makes it beneficial for significance testing in long-term time series data [32]. The formula is as follows:

$$S = \sum_{i=1}^{n-1} \sum_{j=k+1}^{n} Sgn(x_j - x_i) \quad (8)$$

The $Sgn()$ calculation formula is as follows:

$$Sgn(x_j - x_k) = \begin{cases} 1, x_j - x_k > 0 \\ 0, x_j - x_k = 0 \\ -1, x_j - x_k < 0 \end{cases} \quad (9)$$

The formula for the standard normal statistic Z is as follows:

$$Z = \begin{cases} \frac{S}{\sqrt{Var(S)}}, & S > 0 \\ 0, & S = 0 \\ \frac{S+1}{\sqrt{Var(S)}}, & S < 0 \end{cases} \quad (10)$$

The S statistic is as follows:

$$Var(S) = \frac{n(n-1) \times (2n+5)}{18} \quad (11)$$

Using this formula, with a confidence level of $\alpha = 0.05$ and a critical threshold of the statistic Z = 1.96, we will determine whether the trend of LERI is significant. When Z > 1.96, it indicates a significant change; when Z < 1.96, it indicates a significant change, the LERI change trend is divided into five types. That is, when $\beta > 0$ and Z > 1.96, it indicates a significant improvement in LERI; when $\beta < 0$ and Z > 1.96, it indicates a significant degradation of LERI; when $\beta > 0$ and $Z \leq 1.96$, it indicates a slight improvement in LERI; when $\beta < 0$ and $Z \leq 1.96$, it indicates a slight degradation of LERI; other situations indicate that the change in LERI is not significant.

3. Results

3.1. Model Result Analysis

Modeling suitable habitats for three *Tamarix* species was conducted using 143, 173, and 213 distribution records and 13 filtered environmental variables. Spatial sparsity tools were applied to reduce spatial autocorrelation in the data. The ENMeval package was used to select the optimal feature combination and tuning parameters. Simulation prediction

results were evaluated using both AUC and TSS values. The results showed (Table 2) that for *T. chinensis*, *T. austromongolica*, and *T. leptostachya*, the AUC values ranged between 0.9 and 1.0, and the TSS values ranged between 0.8 and 0.9, indicating a high degree of reliability in the predictions.

Table 2. Model accuracy evaluation.

Species	AUC_{train}	AUC_{test}	TSS
T. chinensis	0.933	0.901	0.846
T. austromongolica	0.961	0.943	0.885
T. leptostachya	0.974	0.964	0.862

3.2. Three Types of the Suitable Tamarix Habitat Spatial Pattern Characteristics

The analysis of *Tamarix* habitat areas under current climate models (Figure 2) showed that highly suitable habitats for *T. chinensis*, *T. austromongolica*, and *T. leptostachya* covered 16.83%, 13.29%, and 6.93% of their respective areas, with sizes of 1.88×10^5 km^2, 1.34×10^5 km^2, and 0.78×10^5 km^2, respectively. There was a decreasing trend in highly suitable habitats from east to west, which also applied to moderately and poorly suitable habitats. Unsuitable habitats showed the opposite trend, with *T. chinensis* having the lowest proportion of unsuitable habitat at 18.69% and *T. leptostachya* having the highest proportion at 53.75%. This trend reflected the gradual deterioration of the living environment for these species from east to west in northern China. Figure 3b–d showed the potential distribution simulations of *T. chinensis*, *T. austromongolica*, and *T. leptostachya* under the current climatic conditions, using the MaxEnt model. *T. chinensis* had highly suitable habitats in the Weihe Plain of Shaanxi Province, the Yuncheng Basin–Taiyuan Basin line in Shanxi Province, the northeastern Huang-Huai Plain in Henan Province, the eastern coastal areas and the plain east of the Taihang Mountains in Hebei Province, the southwestern part of Beijing, the central eastern part of Tianjin, the northwestern part of Shandong Province along the Yellow River, and the southern coastal areas of Liaoning Province (Figure 3b). The highly suitable habitats for *T. austromongolica* were located in southern Gansu Province, along the Hexi Corridor, the Hetao Plain, the Heihe River Basin in northwest Inner Mongolia, and the Qaidam Basin in northwest Qinghai Province (Figure 3c). The highly suitable habitats for *T. leptostachya* were found in the northeast and west of the Tarim Basin, with highly suitable areas in the south of the Tarim Basin, distributed along major rivers (Figure 3d). These observations suggested that the suitable habitats for *T. chinensis*, *T. austromongolica*, and *T. leptostachya* were primarily in flat terrains such as plains and basins, indicating a survival advantage in these environments.

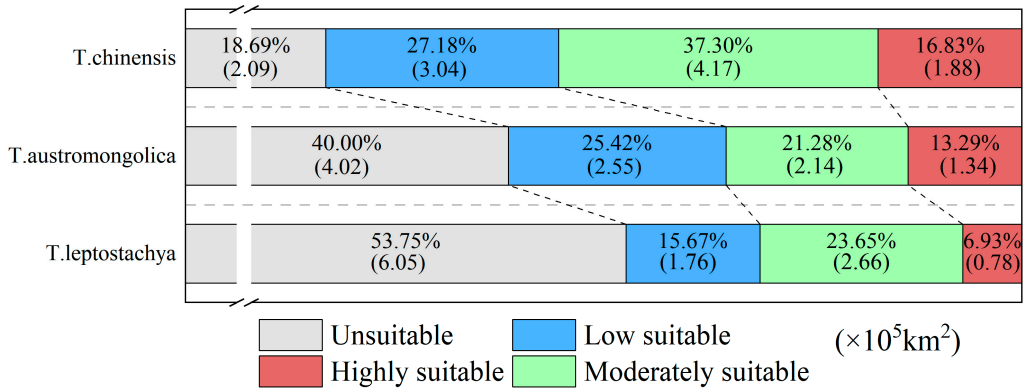

Figure 2. Suitable habitat and proportions of three *Tamarix* L. species.

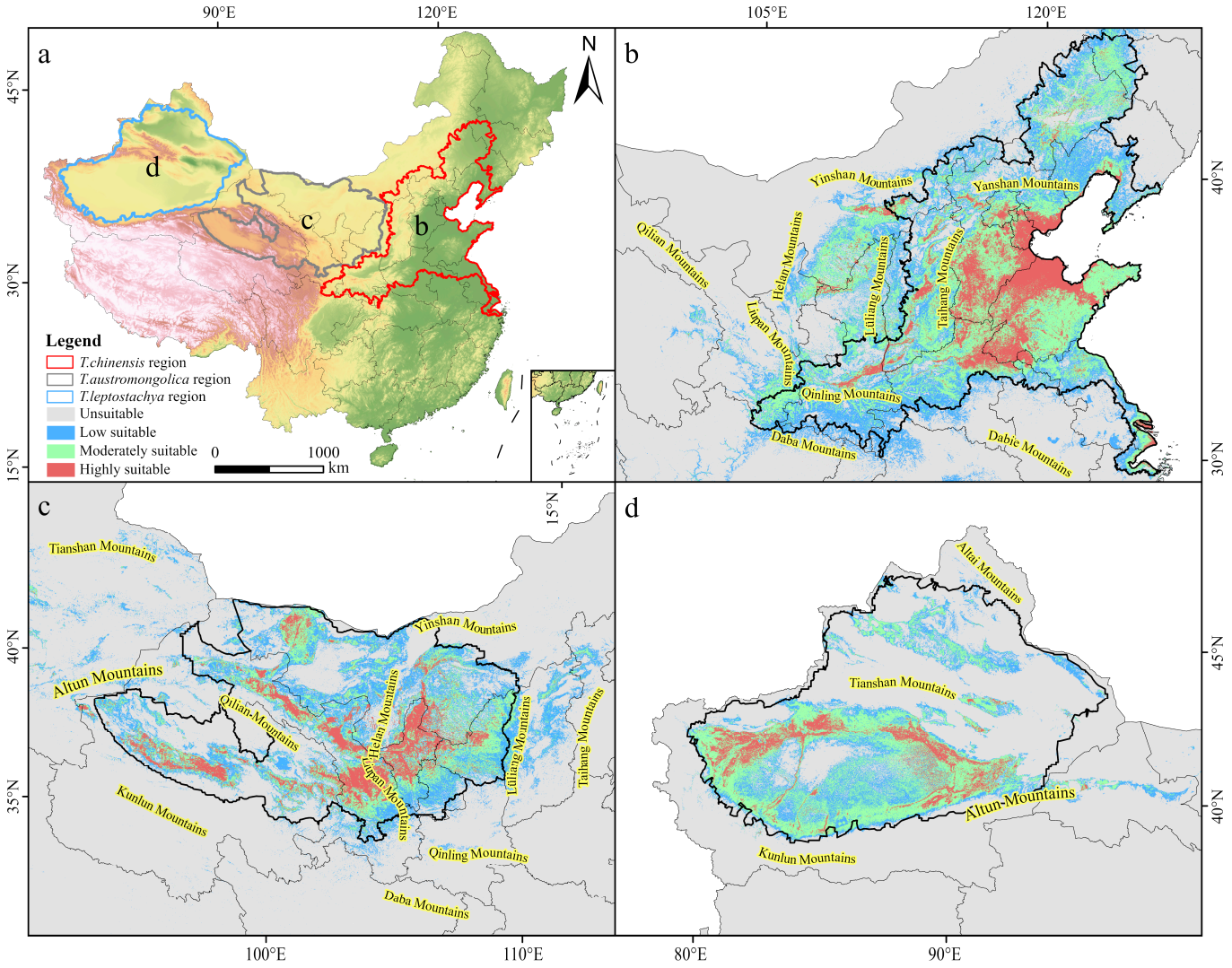

Figure 3. Core potential habitats of the three *Tamarix* species (**a**); and habitat distribution of *T. chinensis* (**b**), *T. austromongolica* (**c**), and *T. leptostachya* (**d**).

3.3. Suitable Habitat Ecological Risk Assessment

This study has constructed the LERI based on land use data from the years 1980, 1990, 1995, 2000, 2005, 2010, 2015, and 2020. Ecological risk values for the core suitable habitats of *T. chinensis*, *T. austromongolica*, and *T. leptostachya* were interpolated using ordinary kriging, and the results were normalized. Using cross-validation with ordinary kriging and simple kriging, the research area LERI for the 1990 dataset was classified into five levels: low-risk area, relatively low-risk area, medium-risk area, relatively high-risk area, and high-risk area, employing the natural breakpoint classification method. For mapping purposes, ecological risk indices from five different periods were selected.

As shown in Figures 4 and 5a–e, the LERI of the core area of *T. chinensis* exhibits a distribution pattern with higher values in the north and west, and lower values in the south and east. Low-risk areas are primarily found along the Changbai Mountains, Yanshan Mountains, Taihang Mountains, Lvliang Mountains, and Qinling Mountains, showing a clear alignment with these mountain ranges. Relatively low-risk areas are mostly located in the eastern plain agricultural regions. Medium-risk areas are mainly in urban and surrounding areas. Higher and high-risk areas are generally near inland wetlands, water bodies, and coastal regions. In the core suitable habitat of *T. chinensis*, the high-risk area in region a_1 has gradually increased and stabilized. This area, the Horqin Sandy Land, is ecologically vulnerable and suffers from severe desertification, which decreases the landscape's resistance

to interference. The low-risk area in region b_1 has continued to expand northeastward, possibly due to Shandong Province's afforestation plan. This predominantly mountainous region, a core area for afforestation in Shandong, has seen reduced landscape fragmentation and increased disturbance resistance. The low-risk area in region c_1 has also expanded due to urbanization around Tai Lake, where construction has replaced original water bodies and farmlands, leading to decreased landscape fragmentation. In region d_1, the low-risk area has become increasingly fragmented, with significant land use changes between 1980 and 2020 contributing to this fragmentation.

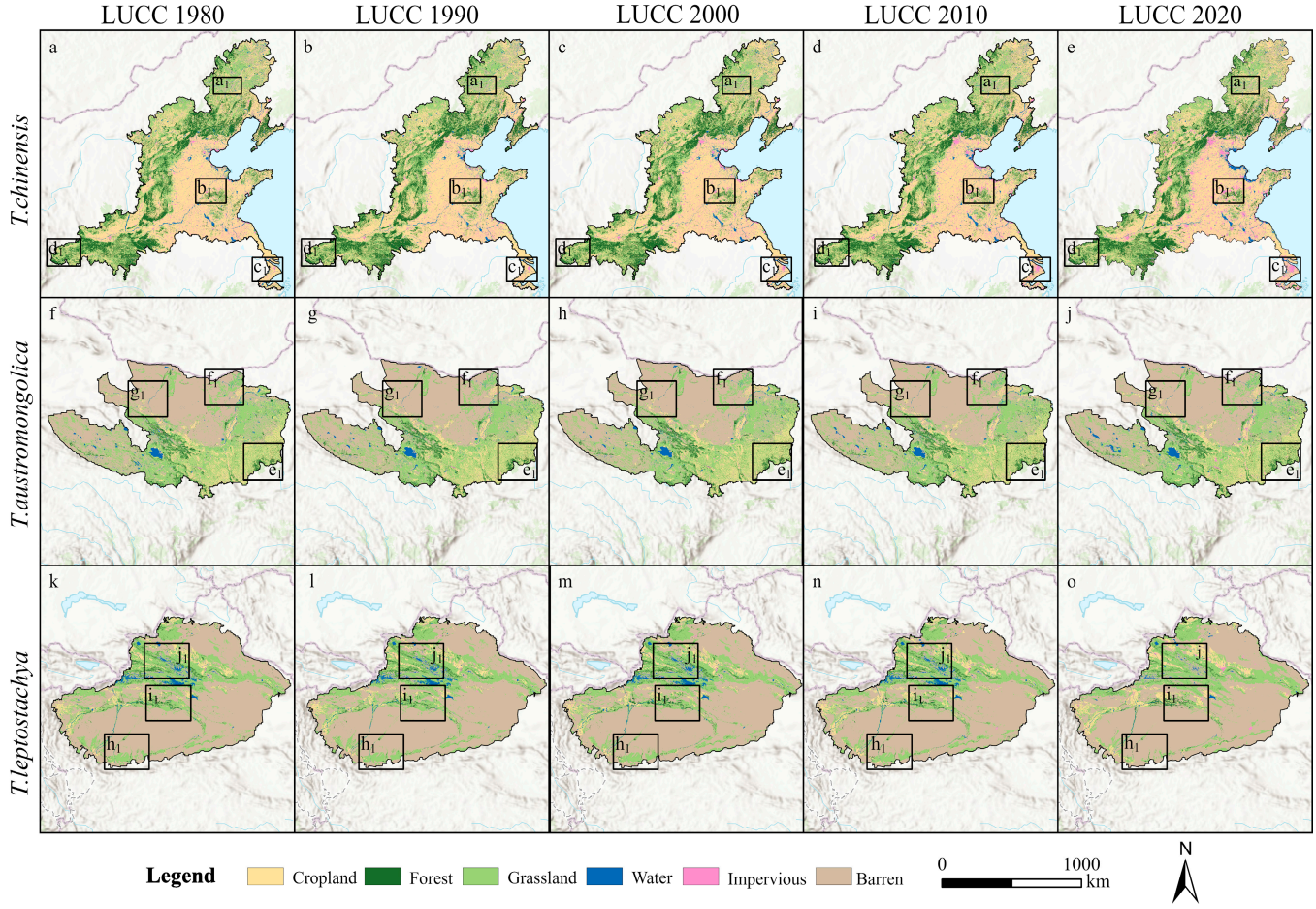

Figure 4. Land use patterns of *T. chinensis* (**a**–**e**), *T. austromongolica* (**f**–**j**), and *T. leptostachya* (**k**–**o**) from 1980 to 2020.

As illustrated in Figures 4 and 5f–j, the LERI of the core area of *T. austromongolica* shows higher values in the southeast and lower values in the northwest. Low-risk areas are concentrated in the eastern Qinghai-Tibet Plateau, east of the Hexi Corridor, and the plains east of the Helan and Liupan Mountains. These low-risk areas are distributed contiguously eastward. Medium-risk areas are primarily found in the northwestern plateau region and southwestern basin areas. Higher- and high-risk areas are mainly located near wetlands and water bodies in the southwestern region. In the core suitable habitat of *T. austromongolica*, the low-risk zone in region e_1 has continued to expand northeastward. Over the past 40 years, increased forest area in this region has reduced landscape fragmentation and improved resistance to disturbances. Region f_1, dominated by grasslands, has faced threats of overgrazing and desertification, leading to a reduction in low-risk areas. In region g_1, higher-risk areas have gradually been replaced by medium-risk areas, resulting in farmland patches becoming more concentrated and continuous. Consequently, the regional LERI has decreased rather than increased.

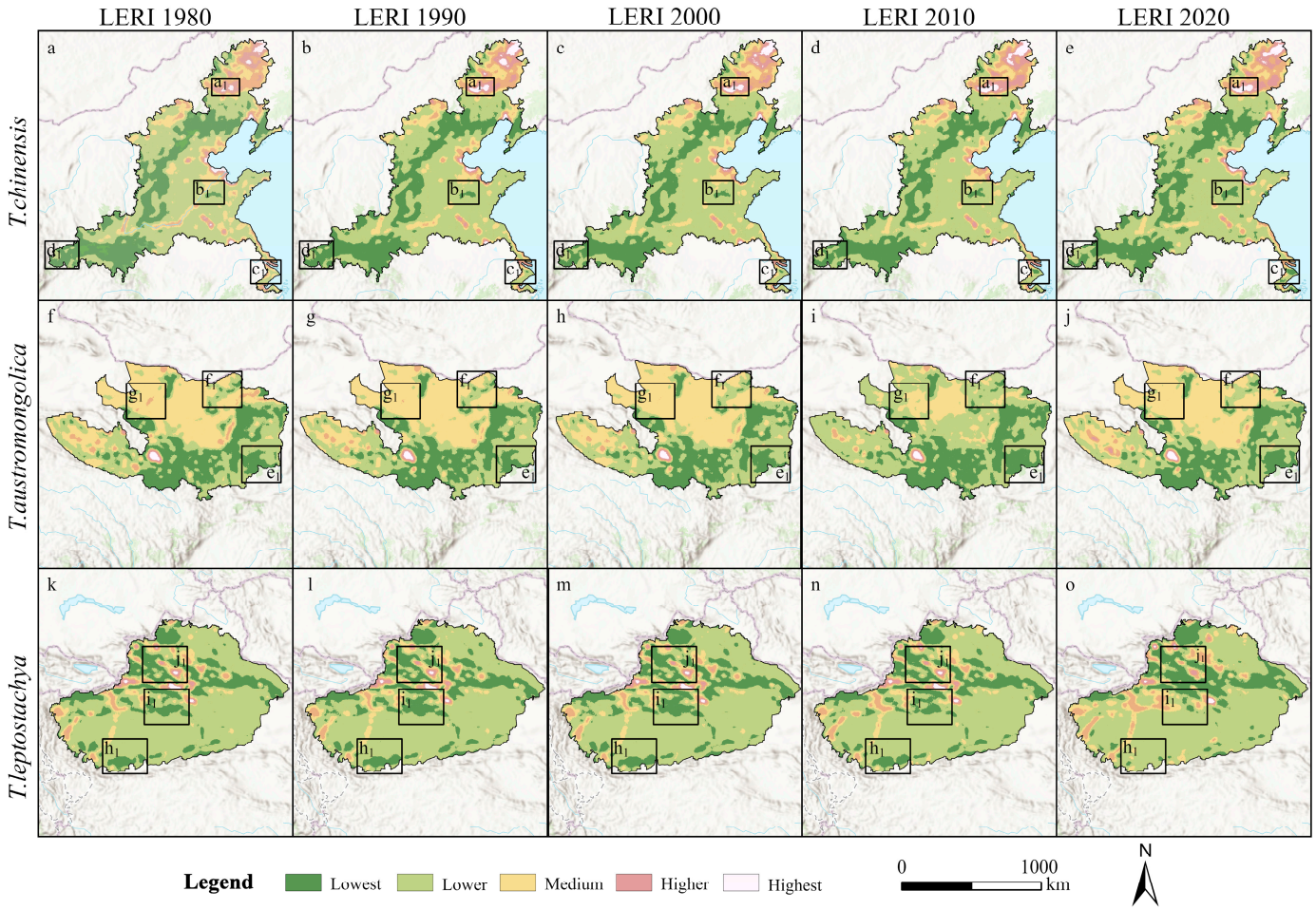

Figure 5. Landscape risk indices for *T. chinensis* (**a**–**e**), *T. austromongolica* (**f**–**j**), and *T. leptostachya* (**k**–**o**).

As shown in Figures 4 and 5k–o, the Landscape Ecological Risk (LERI) in the core area of *T. leptostachya* is lower near mountainous regions and higher in river areas. Low-risk areas are primarily located near the Tianshan Mountains and the northern slopes of the Kunlun Mountains. These lower-risk zones are found in deserts and mountains with minimal human activity. Medium-risk areas are concentrated around cities with frequent human activities. Higher and high-risk areas are mainly situated in central lake regions. In the core suitable habitat of *T. austromongolica*, over the past 40 years, regions h_1 and i_1 have gradually transitioned from grasslands to deserts. This transition has fragmented the grassland landscape, resulting in a continuous reduction in low-risk zones. The LERI in district j_1 has gradually decreased, with a shift from fragmented to concentrated landscapes of cultivated land and water bodies, reducing fragmented patches and increasing landscape dominance.

3.4. Suitable Habitat Ecological Risk Trend Analysis

The Theil–Sen Median trend analysis and Mann–Kendall test were conducted on the ecological risk data from 1980, 1990, 1995, 2000, 2005, 2010, 2015, and 2020 for the core suitable habitats of *T. chinensis*, *T. austromongolica*, and *T. leptostachya* (Figure 6). Over the 40-year period from 1980 to 2020, the core suitable habitat of *T. chinensis* showed a significant upward trend in LERI in the western and northern regions, while areas with significant declines were scattered in the eastern region (Figure 6a). In 1.83×10^5 km^2 of the area, there was a significant increase in LERI ($p < 0.05$), with continuous forests and grasslands being fragmented by cultivated and construction lands, increasing landscape fragmentation and ecological risk. Conversely, 2.21×10^5 km^2 of the area showed a significant decrease in LERI ($p < 0.05$), with reductions resulting in a shift from diverse

land use patterns to dominant land use patterns, decreasing fragmentation, increasing dominance, and enhancing resistance to disturbances. For the core suitable habitat of *T. austromongolica*, areas where LERI increased are primarily in the northwest, with some in the southwest. Regions where LERI decreased are patchily distributed in the east and south (Figure 6b). In 2.68×10^5 km^2 of the area, there was a significant increase in land use efficiency ($p < 0.05$), with deserts and Gobi being the dominant land use types. In 0.81×10^5 km^2 of the area, there was a significant decrease in land use efficiency ($p < 0.05$), with a spatial aggregation trend of forest land, grassland, and cultivated land. For the core suitable habitat of *T. leptostachya*, areas with rising LERI are mainly in the grassland regions of central and northern areas. Patches with significantly declining LERI are located in the Tianshan Mountains and Kunlun Mountains (Figure 6c). In 0.15×10^5 km^2 of the area, there was a significant increase in LERI ($p < 0.05$), indicating that grasslands were being overtaken by desertification. Conversely, a significant decrease in LERI ($p < 0.05$) was observed in 0.24×10^5 km^2 of the area, where deserts were being replaced by cultivated land, thereby enhancing the landscape's resilience to risks.

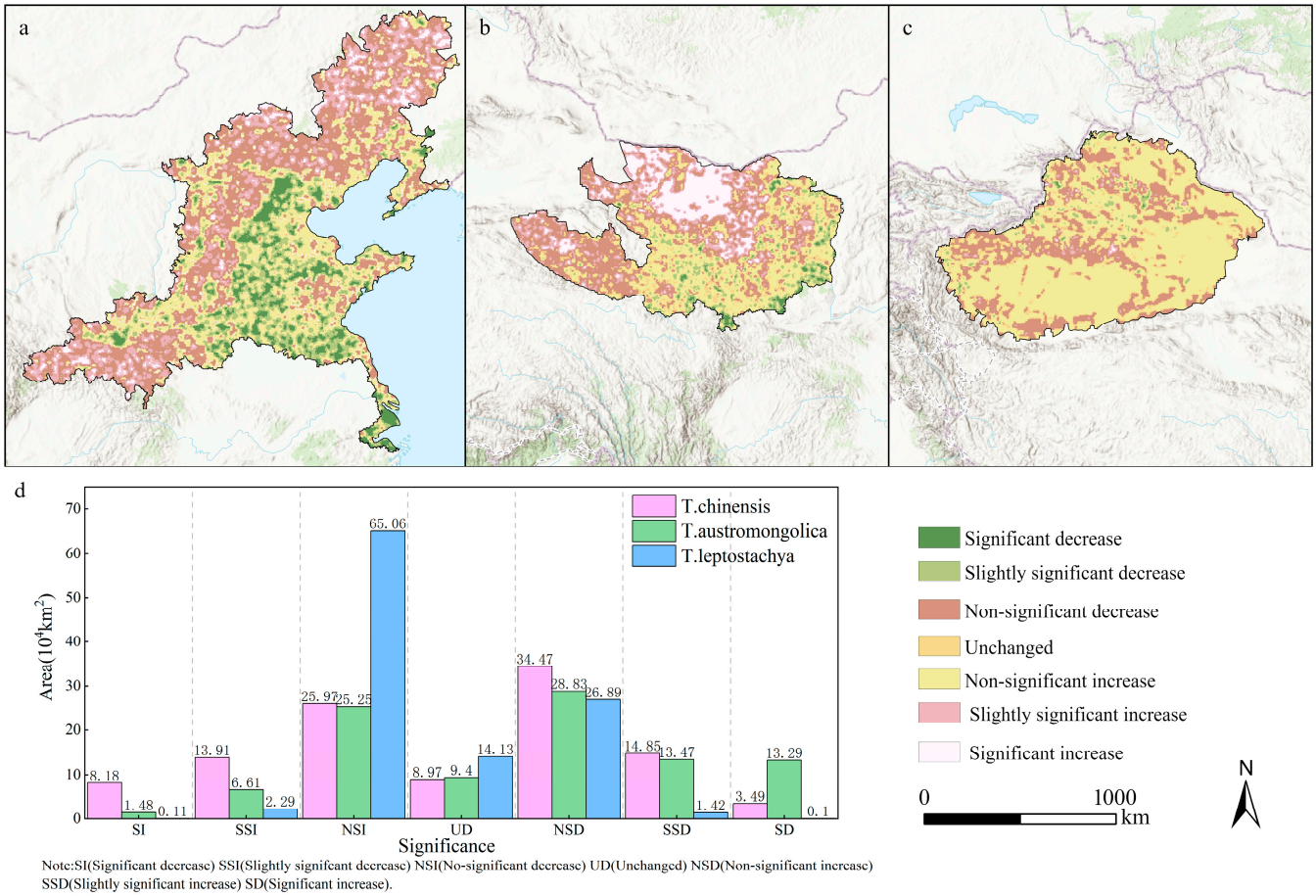

Figure 6. Trends and significance of landscape risk indices for *T. chinensis* (**a**), *T. austromongolica* (**b**), and *T. leptostachya* (**c**); area of significance statistics (**d**).

4. Discussion

4.1. Optimization of Species Suitable Habitats by LERI

The evaluation of species' suitable habitats focuses on studying their geographical distribution patterns and has made significant progress using current climate models and predictions of future suitable habitats [33,34]. Despite variations in data sources, research objectives, driving factors, and scales, most studies use species habitats as a benchmark, but often overlook detailed analyses of suitable habitats under modern climate models [35,36]. Research shows that species' distribution ranges can change rapidly, with a notable trend

towards higher altitudes, latitudes, and inland regions [37,38]. Given the accelerating biodiversity loss, examining the current state of suitable habitats can provide valuable support for species conservation.

Ecological risk research is crucial for preventing ecological deterioration and promoting sustainable development [39]. Although landscape changes are generally slow due to high heterogeneity, spatial components can change at varying speeds and intensities when disturbed. This allows for the assessment of ecological risks through changes in landscape elements, such as risk receptor scope and hazard status [40,41]. Since landscape ecological risk assessments focus on the impact of landscape patterns on ecological processes, they can complement and refine the evaluation of suitable habitats for species [42]. Based on summarizing and reflecting on existing research, we integrated habitat evaluation with LERI. By analyzing LERI characteristics in the study area from 1980 to 2020, we refined the spatial pattern of highly suitable habitats. This approach combines macro-scale habitat evaluation with LERI, offering a more comprehensive assessment of highly suitable habitats for *T. chinensis*, *T. austromongolica*, and *T. leptostachya*. The ecological risks of highly suitable habitats in transition zones between agricultural and pastoral areas, as well as terrain transition zones, require attention.

4.2. Three Types of Tamarisk Suitable Habitat Spatial Distribution Patterns

The highly suitable habitats for three species of Tamarix are primarily distributed in northern China, with the salinized areas of North China and Northwest China serving as their main distribution regions. *T. chinensis* habitats are predominantly in the North China Plain and the Weihe Plain, while *T. austromongolica* is mainly found in the Hetao Plain, Hexi Corridor, and Qaidam Basin. *T. leptostachya* habitats are concentrated on the edge of the Tarim Basin. These *Tamarisk* species are often found in flat terrains with lowland characteristics. LERI results show that most suitable habitats for *T. chinensis* are in areas with lower or above-average risk levels, often near water, though some regions experience soil salinization. Suitable habitats for *T. austromongolica* and *T. leptostachya* are mostly in low-risk areas, with ecological risk requirements increasing from east to west. In the arid and semi-arid desert regions of the west, *Tamarix* plants thrive due to their tolerance to cold, drought, and salinity. In eastern regions, *Tamarix chinensis* dominates coastal wetlands and tidal flats, such as in the Yellow River Delta, where it forms the main vegetation community.

Between 1980 and 2020, ecological risk in the core area of *Tamarix chinensis* showed an increasing trend, with the main areas of concern being the transition zone between the western mountain ranges and the plateau, as well as the northern agro-pastoral ecotone. Complex ecological factors and human impact have exacerbated the risks in these areas, leading to restrictions on the highly suitable habitats of *T. chinensis*. This issue is partly related to the mountainous terrain of the western region and the intense competition among forest trees. The highly suitable habitat of *Tamarix austromongolica* is limited to the northwest desert area outside the Heihe River Basin, where ecological risk is also increasing. This region is extremely arid, and although the genus *Tamarix* is drought-tolerant, its growth is hindered in such extreme conditions. Similarly, the core area of *Tamarix leptostachya* shares characteristics with *T. austromongolica* in terms of climate impact. However, the growth of *T. leptostachya*, which occurs in the extreme arid regions outside the Tarim Basin's river basins, is suppressed. Field investigations have shown that vegetation in the Tarim Basin, far from water sources, requires artificial irrigation to survive. This indicates that although *Tamarix* species are highly adaptable to various ecological environments, their population development is suppressed in areas where ecological risks continue to increase. The areas of increased ecological risk in the core areas where three different types of tamarisks are distributed encompass agricultural and pastoral transition zones with fragile ecological environments, which may affect the regional industrial structure and the development of the agricultural and pastoral industries.

4.3. Limitations and Prospects

Although we have discussed the spatial pattern of suitable habitats for three *Tamarix* species through LERI assessments, human activities were considered less during the MaxEnt modeling and LERI calculation processes, despite their significant role in the ecosystem. Landscape ecological risk assessment relies on empirical parameters to classify the vulnerability of different landscapes, which introduces some uncertainty. There is a lack of quantitative methods to measure the contribution of these driving factors [43].

5. Conclusions

This study assessed the spatial patterns of suitable habitats for *T. chinensis*, *T. austromongolica*, and *T. leptostachya* based on LERI data from 1980 to 2020. The main findings are (1) the high-suitability habitat areas of *T. chinensis*, *T. austromongolica*, and *T. leptostachya* were 1.88×10^5 km^2, 1.34×10^5 km^2, and 0.78×10^5 km^2, respectively, which were concentrated in the flat terrain of plains and basins, confirming their survival characteristics in such environments; (2) the overall spatial pattern of the research area's LERI has remained relatively stable, but, due to changes in the ecological environment and land use practices, ecological risk has increased in the western and northern core areas of *T. chinensis* and the northwestern region of *T. austromongolica*, with an increase in area to 16.70% and 27.22% of the core area, respectively, resulting in a need for strengthened assessment of the ecological risks in these vulnerable zones; (3) areas with significantly increased landscape ecological risks negatively impact the survival environment of *Tamarix*. The highly suitable habitats are spatially separated from regions with increased landscape risks, indicating an urgent need for attention and intervention.

Author Contributions: Conceptualization: F.G.; methodology: F.G. and X.L.; formal analysis: X.C. and Z.M.; writing—original draft preparation: F.G. and J.L. (Jiufen Liu); writing—review and editing: H.L.; funding acquisition: R.L. and R.W.; resources: L.X. and J.L. (Junnan Li). All authors have read and agreed to the published version of the manuscript.

Funding: This work was supported by the Ministry of Natural Resources Key Laboratory of Natural Resources Investigation, the Monitoring and Protection Open Fund Project (No. 2023-B06), Special Funds Projects for Basic Scientific Research Business Expenses of the Chinese Academy of Geological Sciences (Grant No. JKYQN202362), and the Research Fund of the Shanxi Key Laboratory of Geological Disaster Monitoring, Warning and Prevention, Coal Geological Geophysical Exploration Surveying, and the Mapping Institute of Shanxi Province, Grant (No. 2023-S03).

Data Availability Statement: Data will be made available on request.

Conflicts of Interest: The authors declare that they have no conflicts of interest.

References

1. Hassani, A.; Azapagic, A.; Shokri, N. Global predictions of primary soil salinization under changing climate in the 21st century. *Nat. Commun.* **2021**, *12*, 6663. [CrossRef] [PubMed]
2. Liu, L.; Wang, B. Protection of Halophytes and Their Uses for Cultivation of Saline-Alkali Soil in China. *Biology* **2021**, *10*, 353. [CrossRef] [PubMed]
3. Moreira, M.H.; They, N.H.; Rodrigues, L.R.; Alvarenga-Lucius, L.; Pita-Barbosa, A. Salty freshwater macrophytes: The effects of salinization in freshwaters upon non-halophyte aquatic plants. *Sci. Total Environ.* **2023**, *857*, 159608. [CrossRef] [PubMed]
4. Zhang, T.J.; Chen, Y.N.; Ali, S. Abiotic stress and human activities reduce plant diversity in desert riparian forests. *Ecol. Indic.* **2023**, *152*, 110340. [CrossRef]
5. Ben Hsouna, A.; Michalak, M.; Kukula-Koch, W.; Ben Saad, R.; ben Romdhane, W.; Zeljković, S.Ć.; Mnif, W. Evaluation of Halophyte Biopotential as an Unused Natural Resource: The Case of Lobularia maritima. *Biomolecules* **2022**, *12*, 1583. [CrossRef]
6. Cao, Q.Q.; Yang, B.M.; Li, J.R.; Wang, R.S.; Liu, T.; Xiao, H.J. Characteristics of soil water and salt associated with *Tamarix ramosissima* communities during normal and dry periods in a semi-arid saline environment. *CATENA* **2020**, *193*, 104661. [CrossRef]
7. Duan, Q.X.; Zhu, Z.H.; Wang, B.S.; Chen, M. Recent Progress on the Salt Tolerance Mechanisms and Application of Tamarisk. *Int. J. Mol. Sci.* **2022**, *23*, 3325. [CrossRef] [PubMed]

8. Ren, D.; Xu, X.; Ramos, T.B.; Huang, Q.; Huo, Z.; Huang, G. Modeling and assessing the function and sustainability of natural patches in salt-affected agro-ecosystems: Application to tamarisk (*Tamarix chinensis* Lour.) in Hetao, upper Yellow River basin. *J. Hydrol.* **2017**, *552*, 490–504. [CrossRef]
9. Sillero, N.; Arenas-Castro, S.; Enriquez-Urzelai, U.; Vale, C.G.; Sousa-Guedes, D.; Martínez-Freiría, F.; Real, R.; Barbosa, A.M. Want to model a species niche? A step-by-step guideline on correlative ecological niche modelling. *Ecol. Model.* **2021**, *456*, 109671. [CrossRef]
10. Hernandez, P.A.; Graham, C.H.; Master, L.L.; Albert, D.L. The effect of sample size and species characteristics on performance of different species distribution modeling methods. *Ecography* **2006**, *29*, 773–785. [CrossRef]
11. Ahmadi, M.; Hemami, M.-R.; Kaboli, M.; Shabani, F. MaxEnt brings comparable results when the input data are being completed; Model parameterization of four species distribution models. *Ecol. Evol.* **2023**, *13*, e9827. [CrossRef]
12. Bradie, J.; Leung, B. A quantitative synthesis of the importance of variables used in MaxEnt species distribution models. *J. Biogeogr.* **2017**, *44*, 1344–1361. [CrossRef]
13. Radosavljevic, A.; Anderson, R.P. Making better Maxent models of species distributions: Complexity, overfitting and evaluation. *J. Biogeogr.* **2014**, *41*, 629–643. [CrossRef]
14. Xia, J.B.; Lang, Y.; Zhao, Q.K.; Liu, P.; Su, L. Photosynthetic characteristics of *Tamarix chinensis* under different groundwater depths in freshwater habitats. *Sci. Total Environ.* **2021**, *761*, 143221. [CrossRef]
15. Zhang, D.; Yang, W.k.; Pan, B.; Yin, L. Characters of *Tamarix hispida* Willd Communities and Its Ecological & Physiological Adaptation. *J. Desert Res.* **2003**, *23*, 112–117.
16. Yang, W.; Zhang, D.; Yin, L.; Zhang, L. Distribution and Cluster Analysis on the Similarity of the Tamarix Communities in Xinjiang. *Arid Zone Res.* **2002**, *19*, 6–11. [CrossRef]
17. Fang, O.; Jia, H.; Qiu, H.; Ren, H. Age of arboreous *Tamarix austromongolica* and its growth response to environment in Tongde County of Qinghai, China. *Chin. J. Plant Ecol.* **2017**, *41*, 738–748.
18. Hang, F.; Mang, D.; Zheng, Q.; Xiao, B.; Zhang, Y.; Fu, Q.; Du, J. Species Diversity of *Tamarix ramosissima* Communities in DifferentHabitats and the Relationship Between Soil Moisture and Salinityin the Middle and Lower Reaches of Shiyang River Basin. *Res. Soil Water Conserv.* **2022**, *29*, 49–56. [CrossRef]
19. Fick, S.E.; Hijmans, R.J. WorldClim 2: New 1-km spatial resolution climate surfaces for global land areas. *Int. J. Climatol.* **2017**, *37*, 4302–4315. [CrossRef]
20. Xu, D.P.; Zhuo, Z.H.; Wang, R.L.; Ye, M.; Pu, B. Modeling the distribution of Zanthoxylum armatum in China with MaxEnt modeling. *Glob. Ecol. Conserv.* **2019**, *19*, e00691. [CrossRef]
21. Shi, F.N.; Liu, S.L.; An, Y.; Sun, Y.X.; Zhao, S.; Liu, Y.X.; Li, M.Q. Climatic factors and human disturbance influence ungulate species distribution on the Qinghai-Tibet Plateau. *Sci. Total Environ.* **2023**, *869*, 161681. [CrossRef] [PubMed]
22. Xu, L.; Fan, Y.; Zheng, J.H.; Guan, J.Y.; Lin, J.; Wu, J.G.; Liu, L.; Wu, R.; Liu, Y.J. Impacts of climate change and human activity on the potential distribution of Aconitum leucostomum in China. *Sci. Total Environ.* **2024**, *912*, 168829. [CrossRef] [PubMed]
23. Li, S.; Wang, Z.S.; Zhu, Z.X.; Tao, Y.Z.; Xiang, J. Predicting the potential suitable distribution area of Emeia pseudosauteri in Zhejiang Province based on the MaxEnt model. *Sci. Rep.* **2023**, *13*, 1806. [CrossRef] [PubMed]
24. Yang, S.L.; Wang, H.M.; Tong, J.P.; Bai, Y.; Alatalo, J.M.; Liu, G.; Fang, Z.; Zhang, F. Impacts of environment and human activity on grid-scale land cropping suitability and optimization of planting structure, measured based on the MaxEnt model. *Sci. Total Environ.* **2022**, *836*, 155356. [CrossRef] [PubMed]
25. Zhao, X.F.; Lei, M.; Wei, C.H.; Guo, X.X. Assessing the suitable regions and the key factors for three Cd-accumulating plants (Sedum alfredii, Phytolacca americana, and Hylotelephium spectabile) in China using MaxEnt model. *Sci. Total Environ.* **2022**, *852*, 158202. [CrossRef]
26. Shi, X.D.; Wang, J.W.; Zhang, L.; Chen, S.X.; Zhao, A.L.; Ning, X.D.; Fan, G.R.; Wu, N.S.; Zhang, L.; Wang, Z.D. Prediction of the potentially suitable areas of Litsea cubeba in China based on future climate change using the optimized MaxEnt model. *Ecol. Indic.* **2023**, *148*, 110093. [CrossRef]
27. Gao, J.; Gong, J.; Yang, J.X.; Li, J.Y.; Li, S.C. Measuring Spatial Connectivity between patches of the heat source and sink (SCSS): A new index to quantify the heterogeneity impacts of landscape patterns on land surface temperature. *Landsc. Urban Plan.* **2022**, *217*, 104260. [CrossRef]
28. Zhang, Z.; Gong, J.; Plaza, A.; Yang, J.X.; Li, J.Y.; Tao, X.W.; Wu, Z.Y.; Li, S.C. Long-term assessment of ecological risk dynamics in Wuhan, China: Multi-perspective spatiotemporal variation analysis. *Environ. Impact Assess. Rev.* **2024**, *105*, 107372. [CrossRef]
29. Huang, L.Y.; Yuan, L.C.; Xia, Y.Y.; Yang, Z.Y.; Luo, Z.L.; Yan, Z.; Li, M.Y.; Yuan, J.A. Landscape ecological risk analysis of subtropical vulnerable mountainous areas from a spatiotemporal perspective: Insights from the Nanling Mountains of China. *Ecol. Indic.* **2023**, *154*, 110883. [CrossRef]
30. Tan, L.; Luo, W.; Yang, B.; Huang, M.; Shuai, S.; Cheng, C.; Zhou, X.; Li, M.; Hu, C. Evaluation of landscape ecological risk in key ecological functional zone of South–to–North Water Diversion Project, China. *Ecol. Indic.* **2023**, *147*, 109934. [CrossRef]
31. Bal, A. Improving the Robustness of the Theil-Sen Estimator Using a Simple Heuristic-Based Modification. *Symmetry* **2024**, *16*, 698. [CrossRef]
32. Hamed, K.H. Exact distribution of the Mann–Kendall trend test statistic for persistent data. *J. Hydrol.* **2009**, *365*, 86–94. [CrossRef]
33. Xu, H.; Yue, C.; Zhang, Y.; Liu, D.; Piao, S.L. Forestation at the right time with the right species can generate persistent carbon benefits in China. *Proc. Natl. Acad. Sci. USA* **2023**, *120*, e2304988120. [CrossRef]

34. Shabani, F.; Ahmadi, M.; Kumar, L.; Solhjouy-fard, S.; Tehrany, M.S.; Shabani, F.; Kalantar, B.; Esmaeili, A. Invasive weed species' threats to global biodiversity: Future scenarios of changes in the number of invasive species in a changing climate. *Ecol. Indic.* **2020**, *116*, 106436. [CrossRef]
35. Schmidt, H.; Radinger, J.; Teschlade, D.; Stoll, S. The role of spatial units in modelling freshwater fish distributions: Comparing a subcatchment and river network approach using MaxEnt. *Ecol. Model.* **2020**, *418*, 108937. [CrossRef]
36. Sillero, N.; Barbosa, A.M. Common mistakes in ecological niche models. *Int. J. Geogr. Inf. Sci.* **2021**, *35*, 213–226. [CrossRef]
37. Elsen, P.R.; Saxon, E.C.; Simmons, B.A.; Ward, M.; Williams, B.A.; Grantham, H.S.; Kark, S.; Levin, N.; Perez-Hammerle, K.-V.; Reside, A.E.; et al. Accelerated shifts in terrestrial life zones under rapid climate change. *Glob. Chang. Biol.* **2022**, *28*, 918–935. [CrossRef]
38. Barnett, L.A.K.; Ward, E.J.; Anderson, S.C. Improving estimates of species distribution change by incorporating local trends. *Ecography* **2021**, *44*, 427–439. [CrossRef]
39. Xu, W.X.; Wang, J.M.; Zhang, M.; Li, S.J. Construction of landscape ecological network based on landscape ecological risk assessment in a large-scale opencast coal mine area. *J. Clean. Prod.* **2021**, *286*, 125523. [CrossRef]
40. Liu, J.; Xu, Q.L.; Yi, J.H.; Huang, X. Analysis of the heterogeneity of urban expansion landscape patterns and driving factors based on a combined Multi-Order Adjacency Index and Geodetector model. *Ecol. Indic.* **2022**, *136*, 108655. [CrossRef]
41. Wang, S.; Tan, X.; Fan, F. Landscape Ecological Risk Assessment and Impact Factor Analysis of the Qinghai–Tibetan Plateau. *Remote Sens.* **2022**, *14*, 4726. [CrossRef]
42. Salviano, I.R.; Gardon, F.R.; dos Santos, R.F. Ecological corridors and landscape planning: A model to select priority areas for connectivity maintenance. *Landsc. Ecol.* **2021**, *36*, 3311–3328. [CrossRef]
43. Qu, Y.B.; Su, D.S.; Wei, C.C.; Zhang, Q.Q.; Jiang, G.H. How to prevent landscape ecological risk with a land use optimal allocation system: An empirical study of the Yellow River Delta in China. *Ecol. Indic.* **2023**, *154*, 110888. [CrossRef]